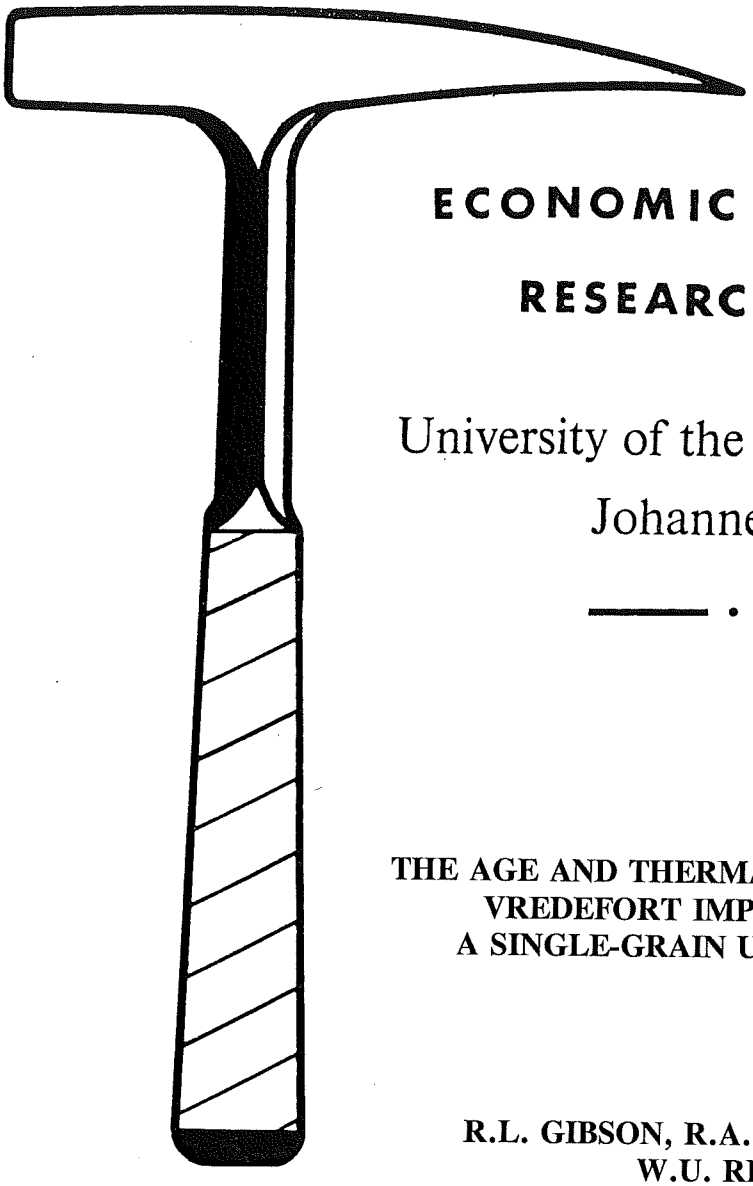

ECONOMIC GEOLOGY
RESEARCH UNIT

University of the Witwatersrand
Johannesburg

THE AGE AND THERMAL EVOLUTION OF THE VREDEFORT IMPACT STRUCTURE: A SINGLE-GRAIN U-Pb ZIRCON STUDY

R.L. GIBSON, R.A. ARMSTRONG AND
W.U. REIMOLD

INFORMATION CIRCULAR No. 309

UNIVERSITY OF THE WITWATERSRAND
JOHANNESBURG

THE AGE AND THERMAL EVOLUTION OF THE VREDEFORT IMPACT STRUCTURE: A SINGLE-GRAIN U-Pb ZIRCON STUDY

by

R.L. GIBSON[1], R.A. ARMSTRONG[2] and W.U. REIMOLD[1]

([1] Department of Geology, University of the Witwatersrand,
P/Bag 3, P O WITS 2050, South Africa)
[2] Research School of Earth Sciences,
The Australian National University,
Canberra 0200 A.C.T. Australia)

ECONOMIC GEOLOGY RESEARCH UNIT
INFORMATION CIRCULAR No. 309

April, 1997

THE AGE AND THERMAL EVOLUTION OF THE VREDEFORT IMPACT STRUCTURE: A SINGLE-GRAIN U-Pb ZIRCON STUDY

ABSTRACT

Single-grain U-Pb SHRIMP analyses of a heterogeneous zircon population from a small granite body in the Archean basement core of the Vredefort Dome indicate an age of 2017 $\pm$ 5 Ma for the granite, which is identical, within errors, to the previously reported age determinations for the Vredefort impact event. Petrographic evidence from the granite indicates that it crystallized after the impact shock event, but some doubt remains whether it is a true impact melt, a decompression melt generated during rapid uplift of the crater basement following the impact event, or a melt generated during an earlier, 2.05 - 2.06 Ga, granulite facies anatectic event that was still at least partially molten at the time of the Vredefort impact event. Rare zircon xenocrysts displaying planar microdeformation features and giving discordant Archean ages are overgrown by polycrystalline zircon rims with U-Th compositions similar to that of the main ~2.02 Ga zircon population, but with discordant $^{207}Pb/^{206}Pb$ ages, indicating more recent Pb-loss.

_____oOo_____

THE AGE AND THERMAL EVOLUTION OF THE VREDEFORT IMPACT STRUCTURE: A SINGLE-GRAIN U-Pb ZIRCON STUDY

CONTENTS

_____oOo_____

Published by the Economic Geology Research Unit
Department of Geology
University of the Witwatersrand
1 Jan Smuts Avenue
Johannesburg 2001
South Africa

ISBN 1 86838 262 1

THE AGE AND THERMAL EVOLUTION OF THE VREDEFORT IMPACT STRUCTURE: A SINGLE-GRAIN U-Pb ZIRCON STUDY

INTRODUCTION

A meteorite impact origin for the Vredefort Dome, an 80 km diameter structure centered at 27° S and 27°30' E some 120 km south-southwest of Johannesburg, South Africa, was first suggested by Boon and Albritton (1936). Despite initial opposition to this hypothesis by some workers (see, for example, references in Nicolaysen, 1990; Reimold, 1993), a large body of evidence has been accumulated in the last 5 years in support of this view (e.g., Reimold and Gibson, 1996). Primarily, this evidence centers around the recognition of shock deformation features, such as shatter cones, coesite and stishovite (high-pressure quartz polymorphs), and planar deformation features (PDFs) developed in quartz and zircon - that indicate the existence of shock pressures in excess of 2 GPa in the rocks of the dome. Additional evidence is provided by clast-laden dykes of an unusual melt rock, the Vredefort Granophyre, which are interpreted as remnants of an impact melt body (Therriault *et al.*, 1996; Koeberl *et al.*, 1996). Other indirect evidence is supplied by the existence of extremely voluminous pseudotachylitic breccias with dimensions of up to several tens to hundreds of meters. These breccias, some of which are spatially and temporally related to shock features (e.g., Reimold, 1990; Martini, 1991; Hart *et al.*, 1991), indicate that the formation of the dome was associated with unusually high strain rate (though not necessarily shock) deformation (e.g., Reimold and Colliston, 1994). Geochronological studies of both the Granophyre (Walraven *et al.*, 1990; Allsopp *et al.*, 1991) and, more recently, the pseudotachylitic breccias (Spray *et al.*, 1995; Kamo *et al.*, 1996) have established an age of ~2.02 Ga for the impact event, making the Vredefort Structure the oldest known impact structure on Earth.

Estimates of the size of the Vredefort impact structure, based on the distribution of the shock features (Therriault *et al.*, 1993) and on geophysical modelling (Henkel and Reimold, 1996), suggest an original diameter of 250 km to >300 km. The Vredefort Dome itself is interpreted as the central uplift of the impact structure, raised by some 10-13 km relative to the outer parts of the structure during the post-impact decompression phase (Henkel and Reimold, 1996; Stevens *et al.*, 1997). Geophysical modelling (Henkel and Reimold, 1996) and geobarometric estimates (Fricke *et al.*, 1990; Stevens *et al.*, 1997) suggest that the dome has been exhumed by a further 6-10 km since the impact event. In contrast, impact structures of comparable size, such as Chicxulub (Sharpton *et al.*, 1992) and Sudbury (Deutsch *et al.*, 1995) are, respectively, still completely buried and not as deeply eroded as Vredefort. Thus, the present exposures in the Vredefort Dome provide a unique opportunity to study the deep levels of a large impact structure.

GEOLOGICAL SETTING

The general geology of the Vredefort Dome is shown in Figure 1. The dome comprises a 45 km diameter core of Archean basement rocks of > 3.1 Ga age (Hart *et al.*, 1981; Kamo *et al.*, 1996) surrounded by a 15-20 km wide collar of steeply dipping to locally overturned supracrustal sequences of Archean to early Proterozoic age (3.07-2.2 Ga). The

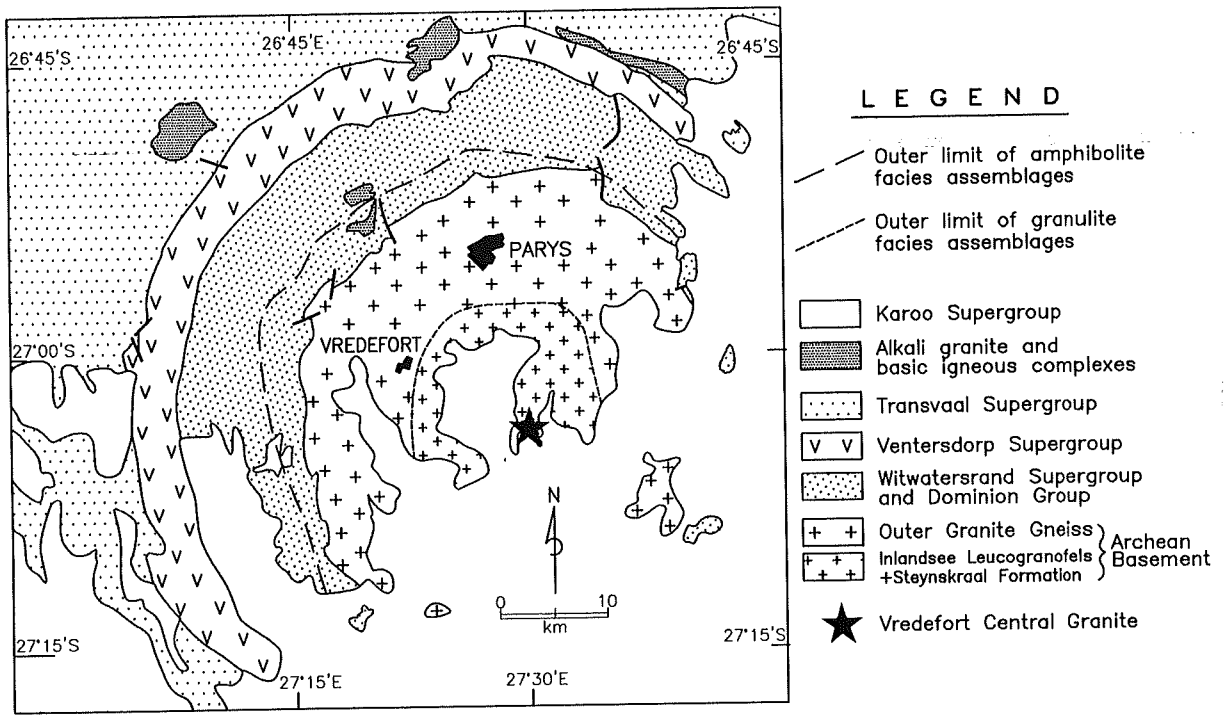

Figure 1: Simplified geological map of the Vredefort Dome showing locality of Vredefort Central Granite.

core is subdivided into an outer annulus of granodioritic to tonalitic gneisses, the Outer Granite Gneiss (OGG), and an inner core dominated by a distinctive leucogranitic gneiss, the Inlandsee Leucogranofels (ILG), which contains xenoliths of predominantly mafic and pelitic Archean greenstone lithologies collectively referred to as the Steynskraal Formation (Stepto, 1979, 1990). Rocks in the core and collar of the dome display a polyphase metamorphic history (e.g., Schreyer, 1983; Stepto, 1990; Gibson and Wallmach, 1995; Stevens *et al.*, 1996), with metamorphic grade increasing from greenschist facies in the outer collar, through mid-amphibolite facies in the inner collar and upper amphibolite facies in the OGG, to granulite facies in the ILG terrain. Although there is general consensus that metamorphic events occurred both prior to and after the shock event and that peak metamorphic grades were attained prior to the shock event, the absolute age and cause of the peak metamorphic event are disputed. Hart *et al.* (1991) proposed that the peak event in the core rocks was Archean in age (> 2.7 Ga), and that the rocks experienced a second thermal event at ca. 2.0 Ga that was induced by the impact event. Recent P-T path work on metapelitic lithologies from the inner collar and the Steynskraal Formation granulites, however, has led Gibson and Wallmach (1995) and Stevens *et al.* (1997) to suggest that the metamorphic peak occurred no more than a few tens of millions of years prior to the impact event, synchronous with the 2.06-2.05 Ga (Walraven *et al.*, 1990; Walraven and Hattingh, 1993; Walraven and Martini, 1995) Bushveld magmatic event. Both Gibson and Wallmach (1995) and Stevens *et al.* (1997) concluded that, due to incomplete cooling of the rocks following this metamorphic peak, the target crust was characterized by an elevated geothermal gradient at the time of the Vredefort impact event and that this played a major role in the post-shock thermal metamorphism in the rocks of the dome.

Central to the debate concerning the relationship between the impact event and the metamorphism in the core rocks is the age and origin of a small occurrence of biotite-bearing leucogranite situated close to the geographic center of the Vredefort Dome (Fig. 1). This granite has been variously referred to as the "Central Intrusive Granite" (Stepto, 1979; Hart *et al.*, 1981), the "Central Anatectic Granite" (Hart *et al.*, 1991), and the "Bullseye granite" (Dence, 1985). Due to the ongoing debate about its origin, we propose the non-genetic name "Vredefort Central Granite". In contrast to the bulk of the lithologies in the dome, including the immediately adjacent ILG gneisses, this granite lacks microscopic shock deformation features in its quartz grains (Hart *et al.*, 1991), suggesting that it crystallized after the impact event. A four-point Rb-Sr whole-rock isochron age of 1950 $\pm$ 60 Ma (Hart *et al.*, 1981) constrains its formation to close to the time of the impact event, now accepted as having occurred at 2023 $\pm$ 4 Ma (single-zircon U-Pb data for unshocked zircons from a pseudotachylitic breccia from the central parts of the dome; Kamo *et al.*, 1996). Based on these limited data, Hart *et al.* (1991) proposed that the granite was derived by partial melting of the underlying ILG as a consequence of crustal heating to pyroxene hornfels facies resulting from the impact event. An impact-related origin for the granite was also proposed by Dence (1985), who interpreted it as an "axial melt" generated during the formation of the central uplift of the impact structure as a result of the combination of impact shock heating and the subsequent rapid uplift of the rocks. He argued that such melts may be characteristic features of the deep levels of large impact structures.

In this paper the authors discuss the implications of new petrographic and SHRIMP (sensitive high-mass resolution ion microprobe) single zircon U-Pb isotopic data for the origin of this granite and its significance for the evolution of the Vredefort Dome.

FIELD AND PETROGRAPHIC RELATIONS

Outcrops of the Vredefort Central Granite occur sporadically over a distance of 4 km in a north-northwest trend along the eastern margin of the Inlandsee Pan within the poorly-exposed ILG gneiss terrain (Fig. 1) (Stepto, 1979). Samples were collected from the largest single outcrop, located at 27° 03' 20" S and 27° 29' 50" E, which comprises several large boulders over an area of no more than 25 m^2 in extent. It was drilled by Hart *et al.* (1991) who concluded that the granite grades downwards at a depth of 10 m into the leucogranofels that constitutes the bulk of the central core of the dome. Stepto (1979) reported apophyses of the granite in contact with spinel-bearing granulite facies paragneisses of the Steynskraal Formation at the northern limits of the outcrop.

The granite is pink, massive, unfoliated, medium-grained, and heterogranular in hand specimen. It comprises K-feldspar (30 vol. %), plagioclase (35 vol. %), quartz (33 vol. %) and biotite (1-2 vol. %) with accessory zircon, apatite and magnetite. Its major element composition, determined by XRF analysis and wet chemistry (for Fe_2O_3), is (values in weight %): SiO_2 = 72.15; TiO_2 = 0.17; Al_2O_3 = 15.33; Fe_2O_3 = 0.84; FeO = 1.10; MgO = 0.4; MnO = 0.02; CaO = 1.82; Na_2O = 3.76; K_2O = 4.34; P_2O_5 = 0.07, indicating a normative composition of Q = 28.9; C = 1.3; Or = 25.7; Ab = 31.8; An = 8.8; Hy = 2.1; M = 1.2; Il = 0.3; Ap = 0.2. Petrographic analysis confirms the lack of foliation in the granite, in contrast to the surrounding leucogranofels and Steynskraal Formation orthogneisses and paragneisses. The micro-texture of the granite is unusual. The feldspar

mineralogy is complex and includes an older generation of perfectly euhedral crystals of plagioclase and orthoclase that are up to 2 mm in length. The plagioclase crystals display a normal zonation. These early-formed feldspars are included in large, anhedral, interlocking crystals (up to 10 mm diameter) of intergranular quartz and patch perthite. The inclusions are generally abundant, producing an almost skeletal texture in the intergranular quartz and perthite crystals. Interstitial granophyric quartz-plagioclase intergrowths are a common feature. The ferromagnesian mineralogy is simple and consists of randomly oriented brown biotite plates up to 6 mm in diameter. Stepto (1979) noted an increase both in the size of the biotite plates (up to 20 mm) and in the biotite content of the granite towards the contact with the spinel paragneiss to the north of the outcrop area. Limited retrogression of biotite to muscovite + chlorite or ilmenite, and of feldspars to sericite, is present.

GEOCHRONOLOGY

Analytical Methods

Zircons were separated and concentrated using conventional heavy liquid and magnetic separation techniques on crushed whole-rock samples. Zircons representing all observed types (discussed below) were mounted in epoxy together with chips of the Research School of Earth Sciences (RSES) standard zircon SL13 (Roddick and Van Breemen, 1994; Claoué-Long *et al.*, 1995) at the Australian National University, Canberra. The zircons were then sectioned approximately in half, polished and photographed. Internal complexities in the zircon growth structures were exposed through cathodoluminescence (CL) imaging. The ability of the SHRIMP ion microprobe to analyse small areas (15-30 μm in diameter) *in situ*, combined with the insights on the zircon structure gained through CL imaging, provides the best possible chance of unravelling the sometimes complex geological history of both individual crystals and heterogeneous populations.

The U-Th-Pb analyses were made on both the SHRIMP I and II instruments at the Research School of Earth Sciences at the Australian National University, Canberra. The data were reduced in a manner similar to that described by Williams and Claesson (1987) and Compston *et al.* (1992). The Pb/U ratios have been normalized to a value of 0.0928 for the $^{206*}Pb/^{238}U$ ratio for the SL13 standard, i.e., equivalent to an age of 572 Ma. U/Pb ages were calculated using the decay constants recommended by Steiger and Jäger (1977) and have been corrected for common Pb using the directly measured ^{204}Pb abundances and the appropriate compositions according to the Cumming and Richards (1975) model. Uncertainties in the isotopic ratios and ages listed in Table 1 and plotted in the figures are one standard error precision estimates based on counting statistics. All final weighted mean ages cited in the text or in the figures are reported with 95% confidence limits.

Results

The zircons extracted from the Vredefort Central Granite are morphologically complex, and it is difficult to make any firm petrogenetic interpretation based solely on their morphology. Prior to SHRIMP analysis, the zircons were categorized on the basis of their morphological characteristics into four types. Type 1 zircons comprise relatively large (up to 400 μm), squat, euhedral to subhedral, crystals which are generally yellow to light brown

Figure 2: Cathodoluminescence image of Type 1 zircon (grain 6). The crystal is composite, comprising a euhedrally-zoned core which has relatively low U and Th concentrations, surrounded by a poorly luminescent overgrowth (outlined by the broken line) with high U and Th contents. The dark irregularly-shaped area in the central part of the crystal is a hole. The areas excavated by the ion probe primary beam are marked (analyses 6.1 and 6.2).

Figure 3: Well-developed sector zoning in a Type 2 zircon as revealed by cathodoluminescence imaging. The grains are clear and apparently unstructured in transmitted light.

Figure 4: Reflected light image of a Type 3 zircon, showing the elongate, prismatic shape, pyramidal terminations and clear, colourless appearance. The core of the grain is metamict and displays radial cracks, and may represent an older grain (see text) or an initial high-U phase of growth during crystallization of the Type 3 zircon. Length of grain 200μm.

Figure 5: Three images of a Type 4 zircon (grain 37). (a) Backscatter electron image showing the ragged, irregular outline of the grain. (b) Differential cathodoluminescence image highlighting the two sets of planar microfractures in the rounded core. Differential CL shows the image by means of enhanced gradients rather than absolute levels, thereby emphasizing internal patterns and boundaries between areas of strongly differing lumination. (c) Cathodoluminescence image showing the complex structure of the grain, with the rounded core mantled by a low-U-Th overgrowth. The planar microfractures are visible as lighter-coloured lines in the core.

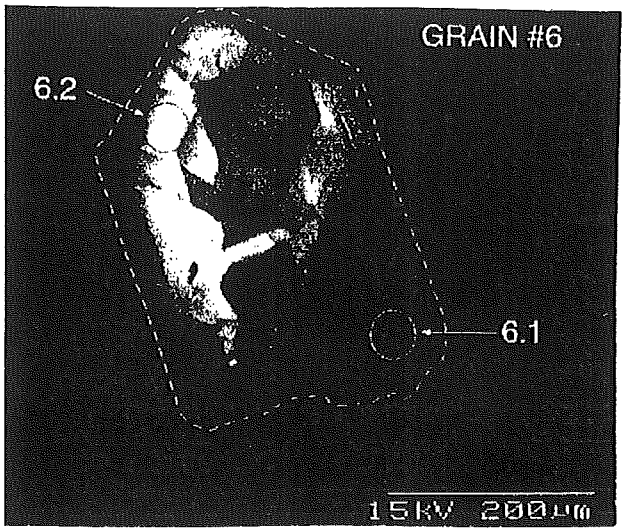

Figure 2

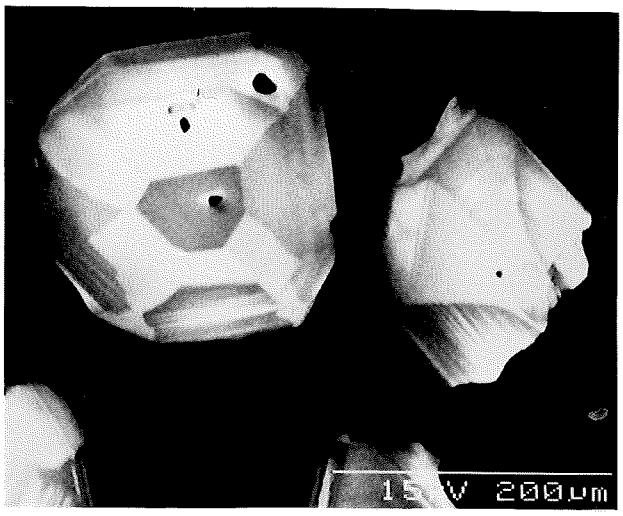

Figure 3

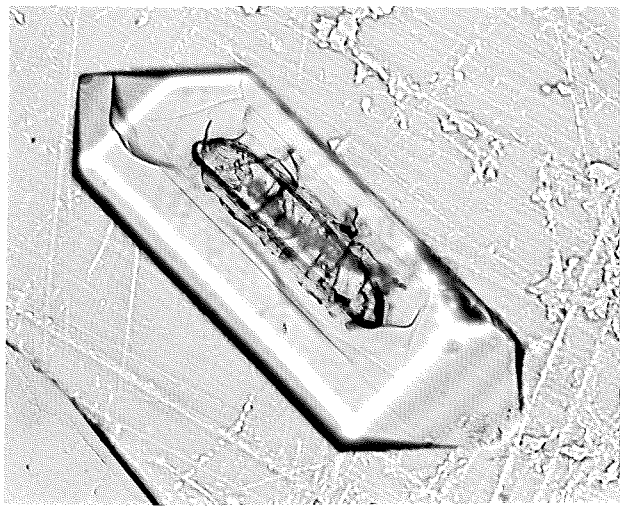

Figure 4

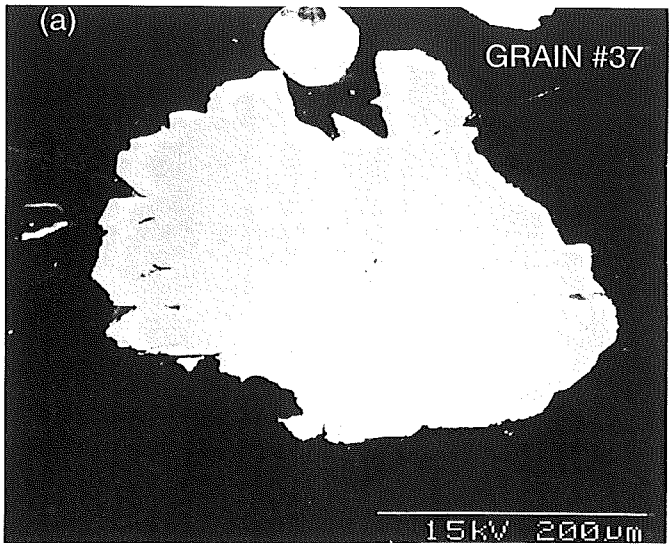

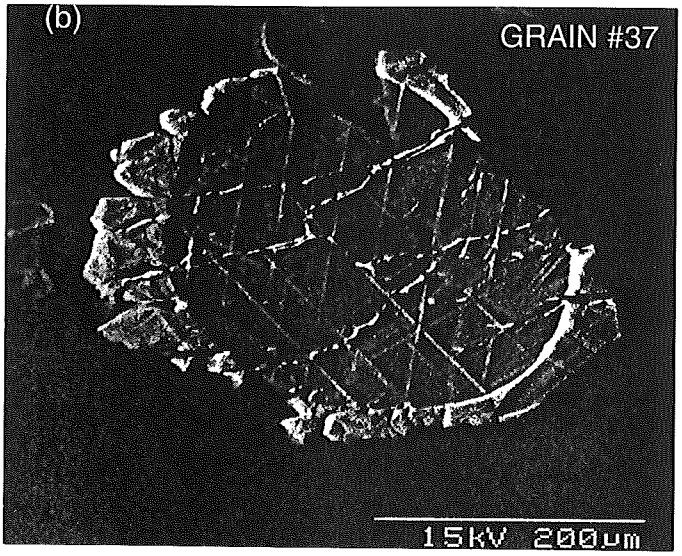

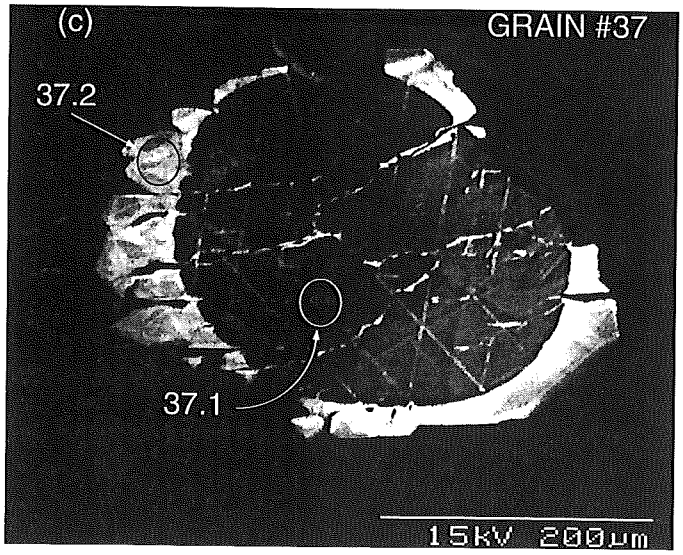

Figure 5

in colour, and some of which are structured into cores and high-U-Th overgrowths (Fig. 2). The cores are strongly zoned and the overgrowths of variable thickness are also strongly zoned and weakly luminescent in CL (Fig. 2). Type 2 zircons are the most abundant sub-population. They are typically 75-200 μm in size and are easily distinguished by their generally well-facetted spheroidal shapes and their clear, colourless, and glassy appearance. In normal transmitted light very little internal structure is seen in these crystals (apart from rare inclusions and holes), but with CL imaging sector zoning of varying complexity is exposed (Fig. 3). Type 3 zircons are also clear, colourless, and glassy in appearance, but they are distinguished from the Type 2 zircons by their elongate, prismatic shape and pyramidal terminations (Fig. 4). They range in length from 50 to 200 μm. Cathodoluminescence imaging shows a range in internal complexity from subtle sector and compositional zoning to simple, uniform, luminescence. The petrogenetic relationships between, and relative ages of, Types 1, 2 and 3 zircons are equivocal.

A number of anhedral rounded crystals with diameters of approximately 300 μm and ragged outlines (Fig. 5a) make up the final sub-population (Type 4). In reflected light, these crystals comprise an opaque central area surrounded by irregular edges of clear zircon. The true complexity and internal detail of the crystals is, however, best observed through CL imaging (Fig. 5b,c). The cores are obviously inherited from some unknown protolith, but what makes them significant is that they display two well-developed sets of regular, planar features (Fig. 5b,c). The clear zircon edges are interpreted as overgrowths precipitated on the rounded cores. The planar features do not appear to extend into the clear zircon edges, indicating that they preceded the overgrowths.

From the listed SHRIMP U-Th-Pb analyses (Table 1) and the concordia plots (Fig. 6a,b) it is clear that some of the complexities observed during zircon characterization are also evident in the U-Pb data. The majority (33 analyses from 29 zircons) of the data, however, plot as a concordant, or slightly discordant, cluster, for which a weighted mean $^{207}Pb/^{206}Pb$ age of 2017 $\pm$ 5 Ma is calculated. These data define a normal Gaussian distribution (Fig. 7) and no statistically significant age differences can be detected between the different sub-populations. This suggests that, although several different morphological types of zircon can be distinguished, in reality there is probably a continuum between these types, reflecting a complex crystallization/metamorphic history.

A number of analyses do not plot in the cluster described above (Figure 6a). These include the two analyses of high-U-Th rims from Type 1 zircons (6.1 and 14.2), which have experienced extreme recent Pb-loss and which are over 90% discordant. Consequently, no meaningful age data could be obtained from these analyses. A number of other discordant analyses (which show the low U and Th contents characteristic of the majority of the zircons from all sub-populations) are distinguished by higher apparent $^{207}Pb/^{206}Pb$ ages (for example, grains 6, 16, 17 and 34, Table 1). These analyses of apparently older zircon suggest the presence of inherited components (either whole grains or parts of grains), which were not detectable by either conventional microscopic or CL imaging, as is obvious for the two Type 4 grains.

Table 1. Summary of ion probe U-Pb results for zircons from the Vredefort Central granite

Grain.area (*)	U (p.p.m.)	Th (p.p.m.)	$\frac{Th}{U}$	^{204}Pb (p.p.b.)	$f^{206}Pb$ (%)	$\frac{^{206}Pb}{^{238}U}$	$\frac{^{207}Pb}{^{235}U}$	$\frac{^{207}Pb}{^{206}Pb}$	AGES (in Ma) $\frac{^{206}Pb}{^{238}U}$	AGES (in Ma) $\frac{^{207}Pb}{^{235}U}$	AGES (in Ma) $\frac{^{207}Pb}{^{206}Pb}$
1.1 (1)	53	87	1.66	3	0.34	0.3380±106	5.721±204	0.1228±17	1877	1935	1997±24
2.1 (1)	87	127	1.46	6	0.34	0.3507±96	5.929±181	0.1226±13	1938	1966	1995±19
3.1 (2)	140	169	1.20	1	0.05	0.3513±90	6.019±164	0.1243± 9	1941	1979	2019±13
4.1 (2)	80	149	1.87	1	0.07	0.3584±98	6.079±178	0.1230± 9	1974	1987	2001±14
5.1 (3)	206	399	1.94	8	0.20	0.3457±89	5.854±163	0.1228± 9	1914	1954	1997±14
6.1 (1)	1040	1942	1.87	92	2.96	0.0515±12	2.762±70	0.3890±30	324	1345	3867±12
6.2 (1)	73	168	2.30	1	0.08	0.3499±92	6.110±178	0.1267±12	1934	1992	2052±17
7.1 (1)	48	86	1.77	6	0.76	0.2962±89	5.930±232	0.1452±31	1673	1966	2290±37
8.1 (2)	84	169	2.01	2	0.15	0.3440±94	5.904±180	0.1245±13	1906	1962	2022±19
9.1 (1)	49	90	1.86	1	0.08	0.3660±107	6.314±211	0.1251±16	2010	2020	2031±23
10.1 (3)	124	256	2.07	0	0.01	0.3420±90	5.868±162	0.1245± 7	1896	1957	2021±10
10.2 (3)	118	259	2.19	1	0.06	0.3596±86	6.181±153	0.1247± 6	1980	2002	2024±8
10.3 (3)	159	334	2.10	5	0.14	0.3663±94	6.266±166	0.1241± 6	2012	2014	2016±8
11.1 (3)	170	347	2.04	2	0.06	0.3517±87	5.959±159	0.1229±10	1943	1970	1999±14
12.1 (2)	60	108	1.81	0	0.02	0.3562±96	6.121±177	0.1246±10	1964	1993	2024±14
13.1 (1)	96	117	1.21	1	0.08	0.3587±96	6.203±179	0.1254±10	1976	2005	2035±14
14.1 (1)	77	157	2.04	37	3.04	0.2726±67	5.067±189	0.1348±34	1554	1831	2162±45
14.2 (1)	1043	1851	1.77	29	1.18	0.0408±15	1.374±52	0.2444±16	258	878	3149±10
15.1 (1)	161	198	1.23	6	0.18	0.3408±80	5.828±145	0.1240± 8	1890	1951	2015±11
16.1 (1)	208	267	1.29	24	0.63	0.3185±78	5.729±154	0.1305±11	1782	1936	2104±15
17.1 (1)	183	337	1.84	41	1.19	0.3283±75	5.845±155	0.1291±14	1830	1953	2086±20
18.1 (3)	96	208	2.15	0	0.02	0.3465±92	5.978±170	0.1251± 9	1918	1973	2030±13
18.2 (3)	89	168	1.89	0	0.02	0.3741±90	6.429±166	0.1247± 8	2049	2036	2024±12
19.1 (3)	73	103	1.41	3	0.21	0.3428±90	5.776±168	0.1222±12	1900	1943	1988±17
19.2 (3)	143	277	1.93	3	0.09	0.3641±92	6.266±167	0.1248± 7	2002	2014	2026±11
20.1 (2)	68	103	1.52	4	0.33	0.3476±108	5.896±219	0.1230±21	1923	1961	2001±30
21.1 (1)	69	98	1.43	7	0.80	0.2150±65	4.057±152	0.1369±26	1256	1646	2188±33
22.1 (2)	65	106	1.63	5	0.40	0.3491±91	5.873±177	0.1220±15	1930	1957	1986±22
23.1 (1)	122	85	0.69	14	1.16	0.1706±43	2.913±101	0.1238±26	1015	1385	2012±38
24.1 (2)	69	156	2.26	3	0.25	0.3387±90	5.740±175	0.1229±15	1881	1937	1999±21
25.1 (3)	48	81	1.68	0	0.02	0.3531±104	6.066±204	0.1246±16	1949	1985	2023±23
26.1 (3)	58	100	1.72	1	0.10	0.3633±95	6.256±176	0.1249±10	1998	2012	2027±14
27.1 (3)	85	129	1.51	3	0.16	0.3627±97	6.177±175	0.1235± 8	1995	2001	2008±12
28.1 (?)	65	108	1.67	1	0.07	0.3658±93	6.247±170	0.1239± 9	2010	2011	2013±13
29.1 (2)	38	71	1.85	1	0.13	0.3699±108	6.261±213	0.1228±17	2029	2013	1997±25
30.1 (2)	44	89	2.01	2	0.21	0.3823±119	6.645±223	0.1261±12	2087	2065	2044±16
31.1 (2)	114	141	1.24	0	0.02	0.3716±98	6.288±172	0.1227± 6	2037	2017	1996±8
32.1 (2)	43	80	1.87	0	0.02	0.3735±107	6.392±200	0.1241±12	2046	2031	2016±18
33.1 (2)	53	91	1.71	2	0.17	0.3732±99	6.334±183	0.1231±11	2044	2023	2002±15
34.1 (3)	52	56	1.09	0	0.02	0.3267±107	5.767±204	0.1280±12	1823	1941	2071±17
35.1 (2)	66	136	2.04	0	0.03	0.3560±92	6.107±167	0.1244± 8	1963	1991	2021±12
36.1 (2)	76	133	1.76	2	0.11	0.3530±99	5.998±186	0.1232±13	1949	1976	2004±18
37.1 (4)	197	307	1.56	10	0.16	0.4866±127	14.155±384	0.2110±11	2556	2760	2913±8
37.2 (4r)	44	95	2.13	23	4.18	0.2118±69	3.473±275	0.1189±81	1239	1521	1940±127
38.1 (4r)	62	110	1.77	12	1.19	0.2786±88	4.692±212	0.1222±35	1584	1766	1988±52
38.2 (4)	103	141	1.36	56	1.94	0.4261±130	11.757±439	0.2001±36	2288	2585	2827±30

Notes: (*) = refers to the zircon type (1, 2, 3 or 4) , with (r) signifying an overgrowth and (?) indicating a zircon which does not fit into this classification; uncertainties are given at the one sigma level; $f^{206}Pb(\%)$ = percentage of total ^{206}Pb which is common ^{206}Pb.

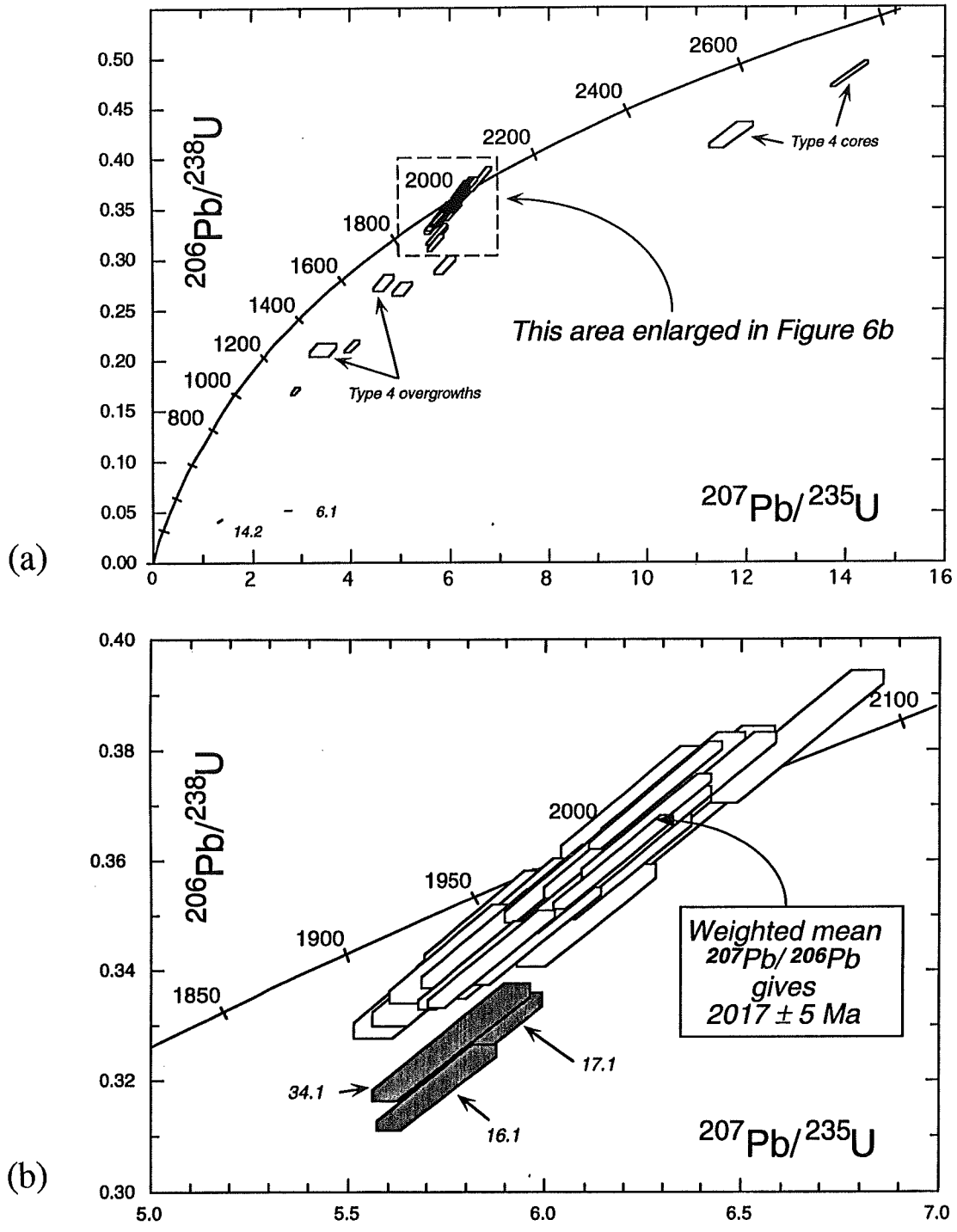

Figure 6: (a) U-Pb concordia diagram showing all the SHRIMP data for zircons from the Vredefort Central Granite (Sample IL2). The error boxes are 1δ and the concordia curve is calibrated in millions of years. Numbers refer to Table 1. (b) Enlarged portion of the U-Pb concordia diagram shown in (a), showing the cluster of data points near concordia from which the weighted mean $^{207}Pb/^{206}Pb$ age of 2017 ± 5 Ma is calculated. The shaded error boxes represent discordant data not included in the age calculation.

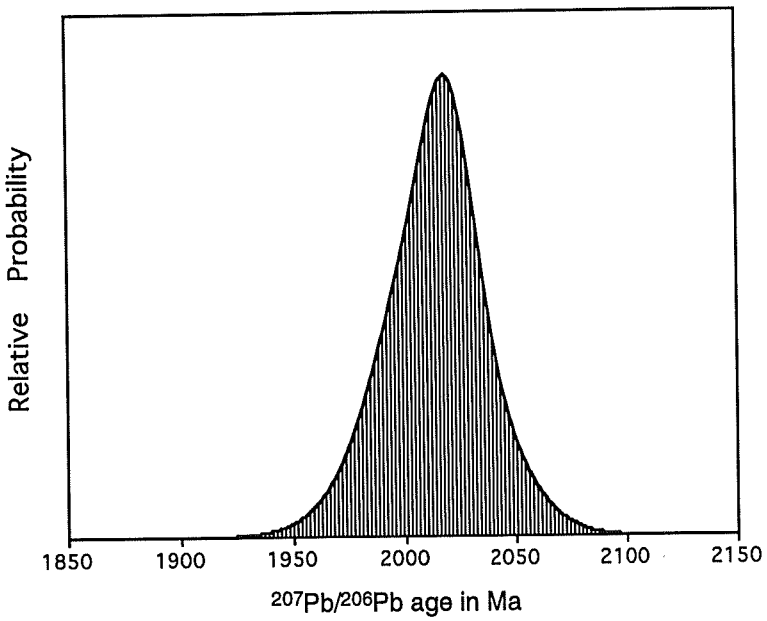

Figure 7: Histogram (Gaussian summation) of $^{207}Pb/^{206}Pb$ ages for the concordant and near-concordant zircon analyses (33 analyses from 29 zircons) from which the mean age was calculated.

Although the data from the two Type 4 zircons (grains 37 and 38, Table 1) are significantly discordant and, hence, do not provide a crystallization age for this rock, they do provide information on the approximate ages of the protolith basement and the overgrowths. The two cores show "ages" of > 2.8 Ga, with the data points showing discordance patterns probably complicated by a combination of recent Pb-loss as well as Pb-loss associated with one or more events at 2 Ga (see below). Similar Pb-loss patterns have been observed in zircons from the Archean basement rocks of the Vredefort Dome core (RAA, unpublished data), and from zircons within pseudotachylitic breccias from the dome (Kamo *et al.*, 1996). The data for the two overgrowths analysed (37.2 and 38.1) are also discordant, but from their U and Th contents and their $^{207}Pb/^{206}Pb$ ages (although imprecise) they appear to belong to the majority 2017 Ma generation of zircons.

DISCUSSION

The Vredefort Central Granite is one of only two lithologies in the core of the Vredefort Dome which does not display evidence of shock-induced planar deformation features in its quartz, the other being the Vredefort Granophyre which is regarded as a *bona fide* impact melt rock (Therriault *et al.*, 1994; Koeberl *et al.*, 1996). This indicates that the crystallization of the Vredefort Central Granite occurred only after the passage of the impact shock wave through the Vredefort basement. The U-Pb age of 2017 $\pm$ 5 Ma obtained in this study is within error of the precise U-Pb zircon age obtained recently by Kamo *et al.* (1996), which they interpret as the age of the impact event, strongly suggesting that crystallization of the Vredefort Central Granite was linked to the impact event. However, the origin of the granite remains problematic.

In the light of the textural and geochronological evidence, three possible explanations exist to account for the genesis of the Vredefort Central Granite:

1. The granite represents a melt produced during the compression phase of the impact event (impact melt, *sensu stricto*);

2. the melt was generated during the decompression phase of the Vredefort impact event; or

3. the melt was produced during a pre-impact high-grade metamorphic event, but it had not yet crystallized by the time of the Vredefort impact event.

All three possibilities require that immediately after the passage of the impact shock wave, temperatures in the rocks in the core of the Vredefort Dome exceeded the minimum granite solidus. At mid- to upper crustal levels, this would imply temperatures in excess of ~650-700 °C (e.g., Thompson and Tracy, 1979).

Theoretical modelling of large meteorite impact structures (e.g., Melosh, 1989) indicates that the magnitude of the post-impact temperatures in the crater basement is related to the combined effects of (a) the original depth of burial of the rocks prior to impact, as a function of the prevailing geothermal gradient, and (b) heat derived from the release of elastic strain energy in the rocks following passage of the shock wave, and from contact metamorphism beneath the impact melt sheet in the crater floor.

The impact melt and decompression melt scenarios require that sufficient heat be produced during the shock event to raise the temperature of the rocks from some sub-solidus pre-impact value to a value at which melting can occur. Single-crystal experiments by Raikes and Ahrens (1979) suggest that, at the shock pressures indicated by the quartz microdeformation features in the rocks in the Vredefort core, post-shock release of elastic strain energy could have resulted in a temperature increase of 150-250 °C (Grieve *et al.*, 1990). Given these figures, published estimates of 15-16 °C/km for the pre-impact geothermal gradient in the rocks of the Vredefort Dome (Grieve *et al.*, 1990; Martini, 1992) appear to be inadequate to account for shock-induced melting, unless the shock heating effect was considerably higher than that suggested by Grieve *et al.* (1990), or the source rocks were derived from deeper crustal levels than is indicated by recent geobarometric estimates (Stevens *et al.*, 1997) and geophysical modelling (Henkel and Reimold, 1996). A more serious problem, however, is the lack of suitable source rocks in the Archean basement to provide a melt at temperatures close to the minimum granite solidus. Experimental studies (e.g., Tuttle and Bowen, 1958) indicate that melting at such temperatures involves breakdown of muscovite, yet it is clear from numerous studies that the Inlandsee Leucogranofels and Steynskraal Formation lithologies experienced a pre-impact granulite facies metamorphism (e.g., Schreyer, 1983; Stepto, 1990; Stevens *et al.*, 1997) which removed muscovite during prograde heating. Consequently, if the formation of the Vredefort Central Granite was triggered by the impact event, it must have formed by dehydration melting of a hydrous phase such as biotite or amphibole in the granulites. Such dehydration melting requires considerably higher temperatures (in excess of 800 °C; Stevens *et al.*, 1995).

If we assume that the extrapolation of the data of Raikes and Ahrens (1979) to the rocks of the Vredefort Dome is valid, a minimum pre-impact geothermal gradient of approximately 25 °C/km would be necessary to effect dehydration melting following the impact shock. Such a value is inconsistent with the estimates of Grieve *et al.* (1990) and Martini (1992); however, it could be explained by an influx of mantle-derived magma into the Kaapvaal crust shortly before the impact event. That such an influx did occur is evidenced by the voluminous mafic-ultramafic magmatism of the Bushveld Complex, which has been dated at 2.05-2.06 Ga (Walraven *et al.*, 1990; Walraven and Hattingh, 1993), approximately 30 Ma prior to the Vredefort event. Although the main remnant of the Bushveld Complex is located approximately 160 km north of the Vredefort Dome, the magmatism did affect the rocks currently exposed in the dome (mafic Bushveld sills occur in the outer collar rocks and the Losberg Complex, which is coeval with the main complex (Coetzee and Kruger, 1989), occurs in the rim synclinorium adjacent to the dome). Significantly, the mafic-ultramafic magmatism is associated with voluminous coeval silicic volcanic and plutonic magmatism (Hatton and Schweitzer, 1995). This magmatism indicates substantial perturbation of the thermal structure of the crust of the Kaapvaal Craton on a regional scale, leading to melting at deep crustal levels. Gibson and Wallmach (1995) and Stevens *et al.* (1997) have recently shown that the P-T paths for the pre-impact amphibolite to granulite facies metamorphism observed in the collar and core rocks of the Vredefort Dome are compatible with a syn-Bushveld Complex timing. They estimated a peak upper- to mid-crustal geotherm of 40-50 °C/km during the magmatothermal event.

As decay to a steady-state geotherm following a thermal perturbation of the magnitude envisaged during the Bushveld Event is likely to have taken at least 60 Ma (e.g., England and Thompson, 1984), it is feasible that the Vredefort impact event occurred in crust characterized by a geothermal gradient that was still significantly elevated. While elevated target-rock temperatures are likely to have enhanced the possibility of melting as a consequence of the impact event, it also raises the possibility that the Vredefort Central Granite represents a melt that was generated during the metamorphic event and that had not yet crystallized by the time of impact.

It is beyond the scope of this paper to enter into a detailed discussion of the behaviour of melts in metamorphic terrains; however, it should be intuitively obvious that such melts could show a range of crystallization ages due to several factors. In the case of melts which segregate and ascend from their source regions to higher, cooler, crustal levels, crystallization may occur relatively soon after the anatectic event. This appears to be the case for the lavas and high-level granites in the Bushveld Complex which show ages within error of the mafic rocks (2.06-2.05 Ga; Walraven *et al.*, 1990; Walraven and Hattingh, 1993; Walraven, 1996). In contrast, *in situ* melt bodies that remain as migmatites in a granulite facies terrain may show crystallization ages that are significantly younger than the melt-forming event, because crystallization will only occur once the rocks have cooled to temperatures below the relevant liquidus. The interval of time which elapses between the metamorphic peak and final melt crystallization will be dependent on both the rate of cooling and the solidus temperature of the melt, which is, in turn, a function of melt composition. Even at cooling rates of 6-10 °C/Ma, which appear to be typical of many metamorphic terrains, it would take in excess of 20 Ma for the rocks to cool from peak metamorphic conditions in the dehydration melting field to below the minimum granite solidus. This has

recently been confirmed by Williams *et al.* (1996) who demonstrated that temperatures in excess of the minimum granite solidus persisted for at least 26 Ma after the attainment of peak metamorphic temperatures in the low-pressure granulite facies Reynolds Range terrain in central Australia.

Stevens *et al.* (1997) have established that peak temperatures achieved in the Steynskraal Formation in the central parts of the Vredefort Dome during the granulite facies event reached 850-920 °C. The restitic compositions of some of these rocks suggest melt extraction, however, other rocks preserve evidence of their melts in migmatitic leucosomes. Some of these leucosomes are cut by pseudotachylitic breccias and contain shock microdeformation features, indicating that they must have crystallized prior to the impact event. Others, however, do not show any such features, and they may contain unusual quench textures indicative of rapid cooling (Fig. 15 in Stevens *et al.*, 1997). Stevens *et al.* (1997) concluded from this that some of the leucosomes were not fully crystalline at the time of the impact event, indicating that the rocks exposed in the central parts of the dome were still at temperatures above the minimum granite solidus some 30 Ma after the metamorphic peak. The Vredefort Central Granite may, thus, represent a melt generated during the pre-impact high-grade metamorphic event that survived until exhumation associated with the impact event triggered rapid cooling of the terrain and consequent crystallization of the surviving melts.

Due to the large uncertainties involved in most of the key parameters relating to the Vredefort impact event, no quantitative modelling of the post-shock thermal effects has yet been attempted. While we favour a Bushveld-related metamorphic origin for the Vredefort Central Granite, the possibility that the granite was generated by the shock event or by decompression melting during the rebound phase of the impact event (Dence, 1985; Hart *et al.*, 1991) cannot, at this stage, be ruled out. Whichever scenario is correct, however, it seems likely that the Vredefort impact occurred into an unusually high-temperature target crust. This has implications for modelling of the Vredefort impact event and for comparison of the Vredefort Structure with other major terrestrial impact structures. Apart from influencing the post-impact thermal evolution of the structure, it may also have implications for the rheological behaviour of the target crust at the time of impact and, consequently, have had an effect on the morphology of the impact structure.

The spaced planar features observed in the cores of the Type 4 zircons in the Vredefort Central Granite bear a strong resemblance to features described by Krogh *et al.* (1984) from the basement of the Sudbury impact structure. Krogh *et al.* (1984) noted visible dislocations along the planes and interpreted them as crystallographically-oriented fractures probably caused by the impact event. These planar features differ from the smaller-scale planar deformation features (PDFs) described in zircons from the K-T boundary distal ejecta by Bohor *et al.* (1993). The features in the K-T boundary ejecta display a similar scale and morphology to the PDFs found in shocked quartz grains and are interpreted as a product of shock-induced melting. Although the spaced fractures and PDFs have, subsequently, been observed together within zircons in the Onaping Formation in the Sudbury Structure (B. Bohor, pers. comm., 1996), a shock origin for the fractures has not been unequivocally proven. Should this prove to be the case, however, the absence of fractures in the overgrowths in the Type 4 zircons from the Vredefort Central Granite provides further

support for a post-shock timing for the overgrowths and, by extension, the low-U-Th zircons constituting the bulk of the zircon population in the granite. Kamo *et al.* (1996) have recently described similar planar features in zircon clasts from the Vredefort Granophyre and pseudotachylitic breccias from the dome. U-Pb data from these zircons indicate original Archean crystallization ages that have been partially reset during the Vredefort Event. Krogh *et al.* (1993a,b) documented progressive Pb-loss associated with shock-induced deformation and recrystallization of zircons from the K/T boundary ejecta and Sudbury Structure. It remains to be seen whether a similar effect is responsible for the slightly discordant ages obtained (Fig. 6a) from the two Type 4 zircons from the Vredefort Central Granite.

If the granite represents a melt that was already present at the time of impact, the presence of planar fractures of possible shock origin in some zircons indicates either that the melt incorporated fragments of shocked wallrocks after the passage of the shock wave, or that the melt was able to transmit the shock stresses into xenocrysts. At the high shock rates expected during impact, the latter scenario may well be feasible, given that the melt would not have been able to escape in the short time that it was subjected to these stresses. Post-shock incorporation of xenoliths cannot be ruled out either, given that the exhumation caused by the impact would have assisted release of dissolved volatiles in the melt due to decompression. This, together with the shock heating effects, could have facilitated additional melting of the wallrocks; however, such melting would need to have been comprehensive as no evidence of other xenoliths has been found in the granite.

CONCLUSIONS

Single-grain U-Pb zircon data from the Vredefort Central Granite indicate a post-shock crystallization age of 2017 $\pm$ 5 Ma for the granite, thus providing further constraints on the age of the Vredefort impact event. Despite the better constraints on the age of the granite, its origin remains ambiguous. It is our opinion that inferences of the deep structure of impact basins based on the exposures in the Vredefort Dome are premature, as the Vredefort Structure may be unusual in having been formed in a relatively 'hot' target crust. Consequently, the presence of granitic melts, represented by the Vredefort Central Granite, in the core of the Vredefort Structure may not be a typical feature of the deep levels of large impact structures.

ACKNOWLEDGEMENTS

Financial support from a University of the Witwatersrand Research Committee Grant (RLG) and a Foundation for Research Development Grant (RLG and WUR) is gratefully acknowledged. The manuscript was greatly improved by discussions with G. Stevens, R. Anderson, B. Bohor, S. Kamo, and C. Koeberl. S. Farrel performed the XRF analysis, J. Aphane assisted with the zircon separation, and S. Stowe and D. Vowles with the zircon images.

REFERENCES

Allsopp, H.L., Fitch, F.J., Miller, J.A. and Reimold, W.U. (1991) $^{40}Ar/^{39}Ar$ stepheating age determinations relevant to the formation of the Vredefort Dome, South Africa. *S. Afr. J. Sci.* **87**, 431-442.

Bohor, B.F., Betterton, W.J. and Krogh, T.E. (1993) Impact-shocked zircons: discovery of shock-induced textures reflecting increasing degrees of shock metamorphism. *Earth Planet. Sci. Lett.* **119**, 419-424.

Boon, J.D. and Albritton, C.C. Jr. (1936) Meteorite craters and their possible relationship to 'Cryptovolcanic Structures'. *Field and Laboratory* **5**, 53-64.

Claoué-Long, J.C., Compston, W., Roberts, J. and Fanning, C.M. (1995). Two Carboniferous ages: a comparison of SHRIMP zircon dating with conventional zircon ages and $^{40}Ar/^{39}Ar$ analysis. In: W.A. Berggren, D.V. Kent, M-P. Aubry and J. Hardenbol (eds.) Geochronology, time scales and global stratigraphic correlation, SEPM (Society for Sedimentary Geology) Special Publication No. 54, 3-21.

Coetzee, H. and Kruger, F.J. (1989) The geochronology and Sr- and Pb-isotope geochemistry of the Losberg Complex, and the southern limit of Bushveld Complex magmatism. *S. Afr. J. Geol.* **92**, 37-41.

Compston, W., Williams, I.S., Kirschvink, J.L., Zhang Zichao, and Guogan, M.A. (1992) Zircon U-Pb ages for the Early Cambrian time-scale. *J. Geol. Soc. London* **149**, 171-184.

Cumming, G.L. and Richards, J.R. (1975) Ore lead isotope ratios in a continuously changing earth. *Earth Planet. Sci. Lett.* **28**, 155-171.

Dence, M.R. (1985) Axial melting in central peaks of complex impact structures. *Meteoritics* **20**, 635-636.

Deutsch, A., Grieve, R.A.F., Avermann, M., Bischoff, L., Brockmeyer, P., Buhl, D., Lakomy, R., Müller-Mohr, V., Ostermann, M. and Stöffler, D. (1995) The Sudbury Structure (Ontario, Canada): a tectonically deformed multi-ring impact basin. *Geol. Rundschau* **84**, 697-709.

England, P.C. and Thompson, A.B. (1984) Pressure-temperature-time paths of regional metamorphism. I: Heat transfer during the evolution of regions of thickened continental crust. *J. Petrol.* **25**, 894-928.

Fricke, A., Medenbach, O. and Schreyer, W. (1990) Fluid inclusions, planar elements and pseudotachylites in the basement rocks of the Vredefort structure, South Africa. *Tectonophys.* **171**, 169-183.

Gibson, R.L. and Wallmach, T. (1995) Low pressure - high temperature metamorphism in the Vredefort Dome, South Africa - anticlockwise pressure-temperature path followed by rapid decompression. *Geol. J.* **30**, 319-331.

Grieve, R.A.F., Coderre, J.M., Robertson, P.B. and Alexopoulos, J. (1990) Microscopic planar deformation features in quartz of the Vredefort structure: Anomalous but still suggestive of an impact origin. *Tectonophys.* **171**, 185-200.

Hart, R.J., Nicolaysen, L.O. and Gale, N.H. (1981) Radioelement concentrations in the deep profile through Precambrian basement of the Vredefort structure. *J. Geophys. Res.* **86**, 10639-10652.

Hart, R.J., Andreoli, M.A.G., Reimold, W.U. and Tredoux, M. (1991) Aspects of the dynamic and thermal metamorphic history of the Vredefort cryptoexplosion structure: implications for its origin. *Tectonophys.* **192**, 313-331.

Hatton, C.J. and Schweitzer, J.K. (1995) Evidence for synchronous extrusive and intrusive Bushveld magmatism. *J. Afr. Earth Sci.* **21**, 579-594.

Henkel, H. and Reimold, W.U. (1996) Integrated gravity and magnetic modelling of the Vredefort impact structure - reinterpretation of the Witwatersrand Basin as the erosional remnant of an impact basin. *EGRU Information Circular, University of the Witwatersrand* **299**, 89 pp.

Koeberl, C., Reimold, W.U. and Shirey, S.B. (1996) A Re-Os isotope study of the Vredefort Granophyre: Clues to the origin of the Vredefort Structure, South Africa. *Geology* **24**, 913-916.

Kamo, S.L., Reimold, W.U., Krogh, T.E. and Colliston, W.P. (1996) A 2.023 Ga age for the Vredefort impact event and a first report of shock metamorphosed zircons in pseudotachylitic breccias and Granophyre. *Earth Planet. Sci. Lett.* **144**, 369-388.

Krogh T.E., Davis D.W. and Corfu F. (1984) Precise U-Pb zircon and baddeleyite ages for the Sudbury area. In: Pye E.G., Naldrett A.J. and Giblin P.E. (eds.) *The Geology and Ore Deposits of the Sudbury Structure*. Ontario Geol. Surv. Spec. Vol. 1, 431-446.

Krogh, T.E., Kamo, S.L. and Bohor, B.F. (1993a) Fingerprinting the K/T impact site and determining the time of impact by U-Pb dating of single shocked zircons from distal ejecta. *Earth Planet. Sci. Lett.* **119**, 425-429.

Krogh, T.E., Kamo, S.L., Sharpton, V.L., Marin, L.E. and Hildebrand, A.R. (1993b) U-Pb ages of single shocked zircons linking distal K/T ejecta to the Chicxulub crater. *Nature* **366**, 731-734.

Martini, J.E.J. (1991) The nature, distribution and genesis of the coesite and stishovite associated with pseudotachylite of the Vredefort Dome, South Africa. *Earth Planet. Sci. Lett.* **103**, 285-300.

Martini, J.E.J. (1992) The metamorphic history of the Vredefort dome at approximately 2 Ga as revealed by coesite-stishovite-bearing pseudotachylites. *J. Metam. Geol.* **10**, 517-527.

Melosh, H.J. (1989). *Impact cratering: a geologic process*. Oxford monographs on geology and geophysics, No. 11, 245 pp.

Nicolaysen, L.O. (1990) The Vredefort Structure: an introduction and a guide to recent literature. *Tectonophys.* **171**, 1-6.

Raikes, S.A. and Ahrens, T.S. (1979) Post-shock temperatures in minerals. *Geophys. J. Royal Astron. Soc.* **58**, 717-747.

Reimold, W.U. (1990) The controversial microdeformations in quartz from the Vredefort Structure, South Africa. *S. Afr. J. Geol.* **93**, 645-663.

Reimold, W.U. (1991) Geochemistry of pseudotachylites from the Vredefort Structure, South Africa. *N. Jahrb. Mineral. Abh.* **161**, 151-184.

Reimold, W.U. (1993) A review of the geology of and deformation related to the Vredefort Structure, South Africa. *J. Geol. Education* **41**, 106-117.

Reimold, W.U. and Colliston, W. P. (1994) Pseudotachylites of the Vredefort Dome and the surrounding Witwatersrand Basin, South Africa. *In* Dressler, B.O., Grieve, R.A.F., and Sharpton, V.L., eds. *Large Meteorite Impacts and Planetary Evolution*, Boulder, Colorado, Geological Society of America Special Paper **293**, 177-196.

Reimold, W.U. and Gibson, R.L. (1996) Geology and evolution of the Vredefort Impact Structure, South Africa. *J. Afr. Earth Sci.* **23**, in press.

Roddick, J.C. and Van Breemen, O. (1994). U-Pb zircon dating: a comparison of ion microprobe and single grain conventional analyses. In: Radiogenic Age and Isotopic Studies. Geological Survey of Canada Current Research 1994-F, Rep. 8, 1-9.

Schreyer, W. (1983) Metamorphism and fluid inclusions in the basement of the Vredefort Dome, South Africa: guidelines to the origin of the structure. *J. Petrol.* **24**, 26-47.

Sharpton, V.L., Burke, K., Camargo-Zanoguera, A., Hall, S.A., Lee, S., Marìn, L.E., Suàrez-Reynoso, G., Quezada-Muñeton, J.M., Spudis, P.D. and Urrutia-Fucgauchi, J. (1992) Chicxulub multiring impact basin: Size and other characteristics derived from gravity analysis. *Science*, **261**, 1564-1567.

Spray, J.G., Kelley, S.P. and Reimold, W.U. (1995) Laser-probe ^{40}Ar-^{39}Ar dating of pseudotachylites and the age of the Vredefort impact event. *Meteoritics* **30**, 335-343.

Stepto, D. (1979) A geological and geophysical study of the central portion of the Vredefort Dome Structure. *Ph.D. thesis, University of the Witwatersrand, Johannesburg*, 642 pp.

Stepto, D. (1990) The geology and gravity field in the central core of the Vredefort structure. *Tectonophys.* **171**, 75-103.

Steiger, R.H. and Jäger, E. (1977) Subcommission on geochronology: convention on the use of decay constants in geo- and cosmochronology. *Earth Planet. Sci. Lett.* **36**, 359-362.

Stevens, G., Clemens, J.D. and Droop, G.T.R. (1995) Hydrous cordierite in granulites and crustal magma production. *Geology* **23**, 925-928.

Stevens, G., Gibson, R.L. and Droop, G.T.R. (1997) Mid-crustal granulite facies metamorphism in the Vredefort Dome: The Bushveld Complex connection. *Precambrian Res.*, in press.

Therriault, A.M. (1992) Field study, petrology and chemistry of the Vredefort Granophyre, South Africa. *M.Sc. thesis, Univ. of Houston, Texas*, 347 pp.

Therriault, A.M., Reid, A.M. and Reimold, W.U. (1993) Original size of the Vredefort Structure, South Africa (abstract). *Lunar Planet. Sci.* **24**, 1419-1420.

Therriault, A.M., Reimold, W.U. and Reid, A.M. (1996) Field relations and petrography of the Vredefort Granophyre. *S. Afr. J. Geol.* **99**, 1-21.

Thompson, A.B. and Tracy, R.J. (1979) Model systems for anatexis of pelitic rocks II. Facies series melting and reactions in the system CaO-$KAlO_2$-$NaAlO_2$-Al_2O_3-SiO_2-H_2O. *Contrib. Mineral. Petrol.* **70**, 429-438.

Tuttle, O.F. and Bowen, N.L. (1958) Origin of granite in the light of experimental studies in the system $NaAlSi_3O_8$-$KAlSi_3O_8$-SiO_2-H_2O. *Geol. Soc. Am. Mem.* **74**, 1-153.

Walraven, F. (1996) Geochronology of the Rooiberg Group, Transvaal Supergroup, South Africa. *Chem. Geol. and Isotope Geosci.*, in press.

Walraven, F. and Hattingh, E. (1993) Geochronology of the Nebo Granite, Bushveld Complex. *S. Afr. J. Geol.* **96**, 31-42.

Walraven, F. and Martini, J. (1995) Zircon Pb-evaporation age determinations of the Oak Tree Formation, Chuniespoort Group, Transvaal Sequence: implications for Transvaal-Griqualand West basin correlations. *S. Afr. J. Geol.* **98**, 58-67.

Walraven, F., Armstrong, R.A. and Kruger, F.J. (1990) A chronostratigraphic framework for the north-central Kaapvaal Craton, the Bushveld Complex and the Vredefort structure. *Tectonophys.* **171**, 23-48.

Williams, I.S. and Claesson, S. (1987) Isotopic evidence for the Precambrian provenance and Caledonian metamorphism of high grade paragneisses from the Seve Nappes, Scandinavian Caledonides. II. Ion microprobe zircon U-Th-Pb. *Contrib. Mineral. Petrol.* **97**, 205-217.

Williams, I.S., Buick, I.S. and Cartwright, I. (1996) An extended episode of early Mesoproterozoic metamorphic fluid flow in the Reynolds Range, central Australia. *J. Metam. Geol.* **14**, 29-47.

_____oOo_____